Cell, Vol. 112, 631–643, March 7, 2003, Copyright ©2003 by Cell Press

Phosphorylation of the AMPA Receptor GluR1 Subunit Is Required for Synaptic Plasticity and Retention of Spatial Memory

Hey-Kyoung Lee,[1,4] Kogo Takamiya,[1,4] Jung-Soo Han,[2] Hengye Man,[1] Chong-Hyun Kim,[1] Gavin Rumbaugh,[1] Sandy Yu,[1] Lin Ding,[1] Chun He,[1] Ronald S. Petralia,[3] Robert J. Wenthold,[3] Michela Gallagher,[2] and Richard L. Huganir[1,*]

[1]Department of Neuroscience
Howard Hughes Medical Institute
Johns Hopkins School of Medicine
Baltimore, Maryland 21205

[2]Department of Psychology
Johns Hopkins University
Baltimore, Maryland 21218

[3]NIDCD
National Institutes of Health
Bethesda, Maryland 20892

Summary

Plasticity of the nervous system is dependent on mechanisms that regulate the strength of synaptic transmission. Excitatory synapses in the brain undergo long-term potentiation (LTP) and long-term depression (LTD), cellular models of learning and memory. Protein phosphorylation is required for the induction of many forms of synaptic plasticity, including LTP and LTD. However, the critical kinase substrates that mediate plasticity have not been identified. We previously reported that phosphorylation of the GluR1 subunit of AMPA receptors, which mediate rapid excitatory transmission in the brain, is modulated during LTP and LTD. To test if GluR1 phosphorylation is necessary for plasticity and learning and memory, we generated mice with knockin mutations in the GluR1 phosphorylation sites. The phosphomutant mice show deficits in LTD and LTP and have memory defects in spatial learning tasks. These results demonstrate that phosphorylation of GluR1 is critical for LTD and LTP expression and the retention of memories.

Introduction

Ionotropic glutamate receptors are the major excitatory neurotransmitter receptors in the vertebrate central nervous system and are divided into three functionally distinct subclasses: AMPA (α-amino-3-hydrozy-5-methylisoxazole-4-propionic acid), kainate, and NMDA (N-methyl-D-aspartate) receptors. AMPA receptors mediate the majority of the fast excitatory synaptic transmission in the central nervous system. Kainate receptors contribute to the postsynaptic responses at some excitatory synapses and can also modulate presynaptic neurotransmitter release. NMDA receptors play an essential role in the modulation of excitatory synaptic transmission due to their permeability to calcium ions and ability to activate downstream calcium-dependent signal transduction processes.

*Correspondence: rhuganir@jhmi.edu

[4]These authors contributed equally to this work.

Synaptic plasticity at excitatory synapses is thought to be critical for information processing in the brain and to underlie many complex behaviors such as learning and memory. The best-studied forms of synaptic plasticity in the central nervous system are long-term potentiation (LTP) and long-term depression (LTD) of excitatory synaptic transmission. The molecular mechanisms of LTP and LTD have been extensively characterized (Malenka and Nicoll, 1999), especially in the hippocampus, an area implicated in spatial memory formation in rodents (Squire, 1992). In the CA1 region of the hippocampus, the induction of LTP and LTD are dependent on NMDA receptor activation and the subsequent increase in intracellular calcium (Malenka and Nicoll, 1999). High-frequency synaptic stimulation leads to the influx of Ca^{2+} through the NMDA receptor and the activation of calcium/calmodulin-dependent protein kinase II (CaMKII) and the induction of LTP. In contrast, low-frequency synaptic stimulation causes moderate, prolonged increases in calcium levels that activate protein phosphatases and leads to LTD. The key substrates for the kinases and phosphatases that mediate the changes in synaptic transmission during LTP and LTD are unknown. A variety of evidence has indicated that changes in both the presynaptic release of glutamate and changes in the postsynaptic response to glutamate are involved in the expression of LTP and LTD (Malenka and Nicoll, 1999). Recent studies, however, indicate that LTP and LTD may be expressed, in part, by regulation of AMPA receptor function (Song and Huganir, 2002). The regulation of AMPA receptor function occurs through two distinct but interrelated mechanisms: modulation of ion channel properties of the receptor and regulation of the synaptic targeting of the receptor (Benke et al., 1998; Hayashi et al., 2000; Shi et al., 2001, 1999). Both of these processes are regulated by protein phosphorylation of the receptor (Song and Huganir, 2002). AMPA receptors are tetramers comprised of a combinatorial assembly of four subunits, GluR1–GluR4. The subunit composition of AMPA receptors varies, depending on the expression patterns of the four subunits in the CNS (Boulter et al., 1990; Keinanen et al., 1990; Martin et al., 1993; Petralia and Wenthold, 1992). There are ten identified phosphorylation sites on the intracellular carboxy-terminal domains of GluR1–GluR4 (Carvalho et al., 1999; Chung et al., 2000; Matsuda et al., 1999; McDonald et al., 2001; Roche et al., 1996). The functional role of phosphorylation of two sites on the GluR1 subunit, serine 831 (S831) and serine 845 (S845), has been extensively characterized. S831 is phosphorylated by CaMKII and protein kinase C (PKC), while S845 is phosphorylated by cAMP-dependent protein kinase (PKA) (Barria et al., 1997a; Mammen et al., 1997; Roche et al., 1996). Phosphorylation of either of these two sites potentiates AMPA receptor ion channel function (Banke et al., 2000; Barria et al., 1997a; Derkach et al., 1999; Roche et al., 1996). Previous studies indicate that phosphorylation of these sites on the GluR1 subunit of AMPA receptors changes with LTP and LTD induction, consistent with a role for GluR1 phosphorylation in the expression of LTP and LTD (Bar-

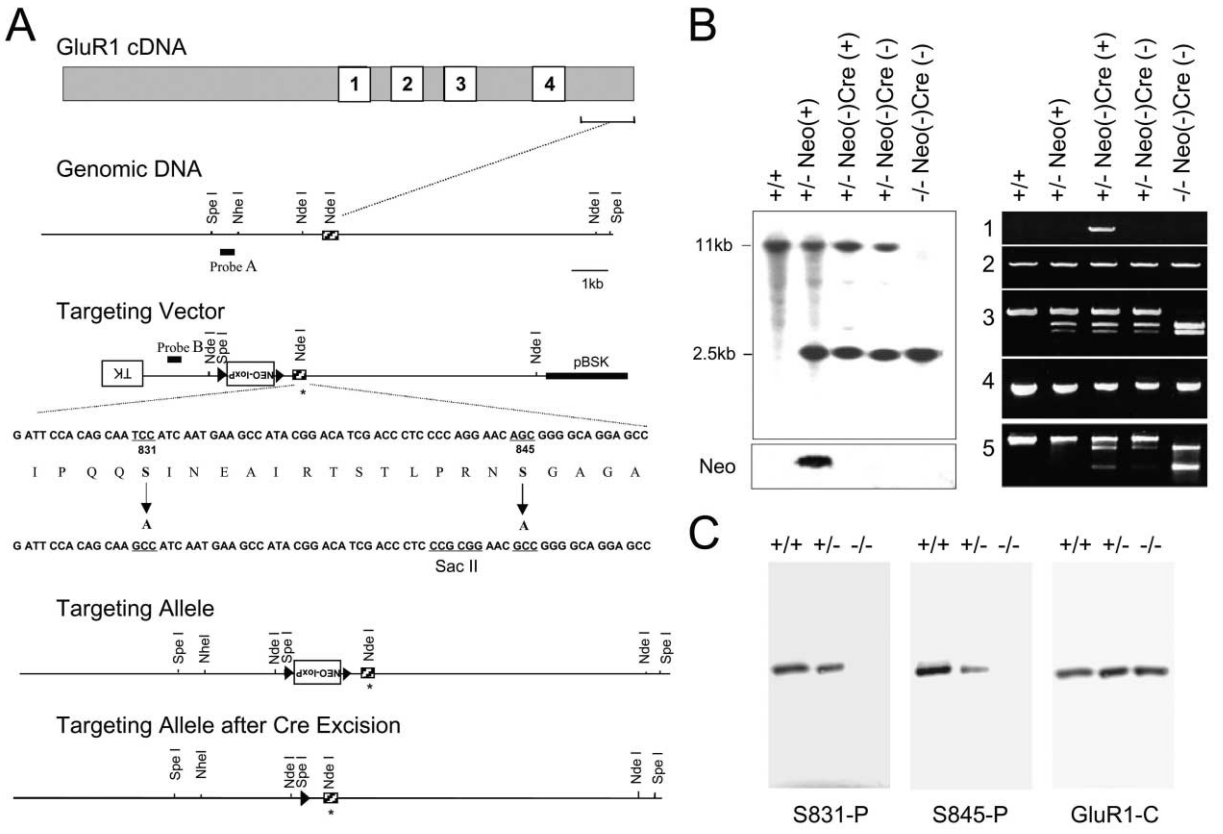

Figure 1. Generation of GluR1 Double Phosphomutant Mice

(A) Top: schematic representation of the GluR1 protein structure (transmembrane domains labeled 1, 2, 3, 4). Middle: genomic DNA structure with the relevant restriction enzyme sites; slashed box represents exon 17 encoding the carboxy-terminus of GluR1. Bottom: targeting vector. TK, thymidine kinase gene; *Neo*-loxP, PGK promoter neomycin-resistance gene with loxP sequence at both sides. The alanine substitution for serine and silent Sac II site to distinguish mutation are shown in lower panel. The probes A and B, which contain the genomic sequence outside and inside of targeting vector, respectively, are depicted as solid bars.

(B) Top left: genomic Southern blot from mice tail samples digested with Spe I and hybridized with probe A. Wild-type (+/+), heterozygote (+/−), homozygote (−/−), and the existence of neomycin-resistant gene (*Neo*) and *cre* gene (*Cre*) are indicated. Bottom left: genomic Southern blot using the same sample indicated in upper panel probed with the probe of neomycin resistant gene coding region. Right: PCR analysis of indicated samples (genomic DNA; 1 and 2, cDNA; 4 as templates). PCR for *cre* gene (1) and mutation site (2) and restriction enzyme digested results of 2 by Sac II (3). RT-PCR results of each genotype (4) and restriction enzyme digested results of 4 by Sac II (5).

(C) Absence of phosphorylation at S831 and S845 in double phosphomutants. Hippocampal samples from wild-type (+/+), heterozygote (+/−), and homozygote (−/−) were prepared for immunoblot analysis using phosphorylation site-specific Ab's against S831 (left) and S845 (middle) or GluR1-carboxy tail Ab (right). Note that phosphorylation signal is absent in homozygotes, while GluR1 expression level (GluR1-C) is normal.

ria et al., 1997b; Kameyama et al., 1998; Lee et al., 2000, 1998). LTP is associated with an increase in phosphorylation of GluR1 (Barria et al., 1997b; Lee et al., 2000), and LTD is correlated with a dephosphorylation of GluR1 (Kameyama et al., 1998; Lee et al., 2000, 1998). Interestingly, the specific phosphorylation site modulated during LTP and LTD is dependent on the history of synaptic plasticity. For instance, in naïve synapses LTP induction increases phosphorylation on S831 (Barria et al., 1997b; Lee et al., 2000), while in previously depressed synapses LTP induction increases phosphorylation on S845 (Lee et al., 2000). Similarly, LTD induction in naïve synapses results in the dephosphorylation of S845, while LTD induction in previously potentiated synapses leads to the dephosphorylation of S831 (Lee et al., 2000). However, the exact role of these phosphorylation events in the expression of LTP and LTD remains unclear.

Here, we report the generation of mutant mice in which both S831 and S845 on GluR1 are mutated to alanines using gene knockin techniques to prevent phosphorylation of these sites in vivo. Using the GluR1 "phospho-free" mice, we tested if phosphorylation of these two sites is necessary for LTD and LTP expression and analyzed the potential role of these phosphorylation sites in learning and memory. We find that the GluR1 double phosphomutant mice essentially lack NMDA receptor-dependent LTD and show reduced LTP in the CA1 region of the hippocampus. These changes were not due to alterations in gross anatomy or normal basal synaptic transmission. In addition, the mice have a defect in the retention, but not learning, of a spatial memory task using the Morris water maze. These results identify a critical protein kinase and phosphatase substrate that mediates synaptic plasticity and demonstrates that the

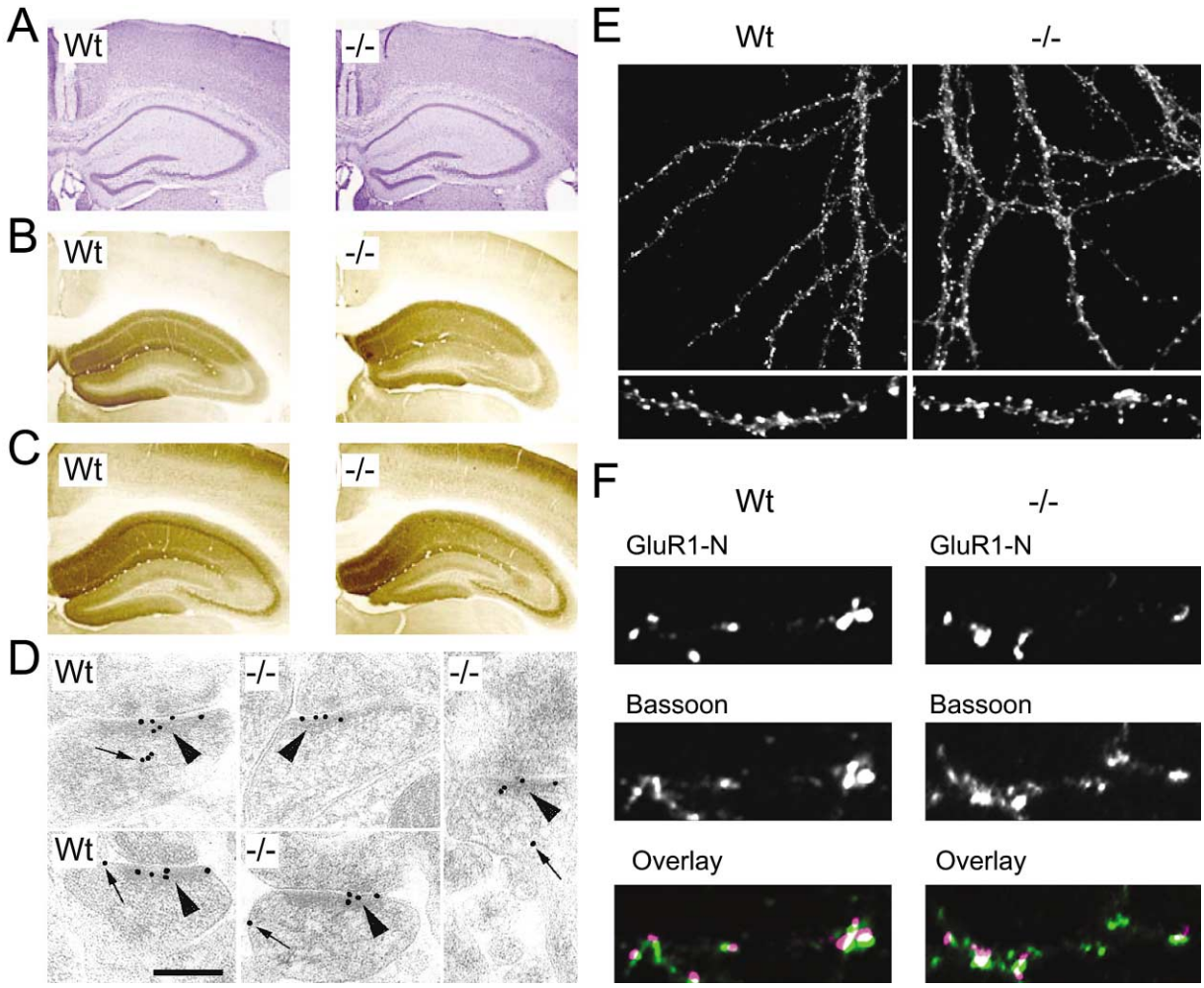

Figure 2. Normal Gross Anatomy and Distribution of GluR1 and GluR2/3 Subunit in the Hippocampus and at Synapses in the Double Phosphomutant Mice

(A) Nissl-stained sections of hippocampus from wild-type (Wt) and homozygote (−/−), showing no gross abnormalities in the cytoarchitecture.
(B) Normal distribution of GluR1 in the hippocampus of homozygote (−/−) compared to the wild-type (Wt) as shown by immunohistochemical staining of brain sections with α-GluR1C Ab.
(C) Similar distribution of GluR2/3 subunit of AMPA receptors in wild-type (Wt) and homozygote (−/−) hippocampus. The brain sections were stained with α-GluR2/3C Ab.
(D) Immunogold labeling of GluR1 in the CA1 stratum radiatum region of the hippocampus of wild-type and mutant mice. Note that GluR1 subunit is distributed at the postsynaptic densities (PSDs) in both wild-type (Wt) and homozygote (−/−). The closed arrowheads point to gold particles localized in PSDs. The narrow arrows point to peri-/extra-synaptic labeling and labeling in spine cytoplasm. The calibration bar is 0.2 μm.
(E) GluR1 is localized at synapses in both wild-type (Wt) and homozygote (−/−) as shown in cultured hippocampal neurons labeled with α-GluR1-N Ab after permeabilization.
(F) Surface GluR1 staining (magenta) overlaps with a presynaptic protein Bassoon (green) in both wild-type (Wt) and homozygote (−/−). Cultured hippocampal neurons were stained live with α-GluR1-N Ab, then fixed, permeabilized, and stained using α-Bassoon Ab.

phosphorylation of the AMPA receptor GluR1 subunit is required for LTD and LTP expression and spatial memory retention.

Results

Generation of GluR1 Phosphorylation Site Mutant Mice

To directly test the role of AMPA receptor GluR1 phosphorylation in bidirectional synaptic plasticity and in learning and memory, we generated a line of mutant mice that lack the two major GluR1 phosphorylation sites (double phosphomutant mice). The mice were generated by introducing mutations at the two phosphorylation sites in the mouse GluR1 gene using homologous recombination techniques (knockin technique). A targeting vector encoding alanine substitutions at the two major phosphorylation sites, S831 and S845, in exon 17 was constructed with a lox-P flanked neomycin resistant (*neo*^{r}) marker in intron 16 (Figure 1A). Correctly targeted ES cells containing the alanine mutations and *neo*^{r} cassette were injected into C57BL/6 blastocysts. Chimera

mice carrying the mutant allele were bred to C57B/6 mice to generate heterozygous mice (GluR1 double mutant +/−, *neo*[+]). Heterozygous mice were then bred to CMV-*Cre* mice to delete the *neo*^{r} cassette from the germ line via the *cre*-loxP system (Nagy et al., 1998) and then intercrossed to produce the double phosphomutant homozygous mice. The success of these procedures was confirmed by Southern blot and PCR analysis (Figure 1B). The GluR1 phosphorylation mutant mice showed no overt behavioral phenotype and bred normally.

We confirmed the mutation of two phosphorylation sites by immunoblot analysis using phosphorylation site-specific antibodies. Detection of GluR1 by the phosphospecific antibodies to S831 and S845 was completely absent in the homozygotes and was about half the level of wild-type in the heterozygotes (Figure 1C). In contrast, the expression of GluR1 subunit detected by anti-GluR1 carboxy-terminal (α-GluR1-C) antibodies was normal (Figure 1C), indicating that the targeted GluR1 gene expresses the GluR1 protein at normal levels. Nissl-stained brain sections from homozygous mice did not show any gross abnormalities in cytoarchitecture compared to the wild-types (Figure 2A). The distribution of both GluR1 and GluR2/3 in the double phosphomutant mice was comparable to that in the wild-types when compared by immunohistochemical staining of brain sections using anti-GluR1 antibody (α-GluR1-C) and anti-GluR2/3 (α-GluR2/3-C) antibodies (Figures 2B and 2C). To confirm that the mutated GluR1 is delivered to the postsynaptic membrane, we performed immunogold electron microscopy with α-GluR1-C antibodies. Similar levels of gold particles were found at the postsynaptic density (PSD) in wild-type (0.71 $\pm$ 0.07 particles/synapse, n = 4 mice) and in the double phosphomutants (0.61 $\pm$ 0.10 particles/synapse, n = 4 mice; Student's t test, $p > 0.4$) in the CA1 region (Figure 2D). In addition, primary cultures of hippocampal neurons from both wild-type and homozygous mice contain punctate staining with GluR1 antibodies under permeabilized (labels all GluR1, Figure 2E) and nonpermeabilized (labels only the surface GluR1; Figure 2F) conditions. Moreover, the surface GluR1 clusters colocalized with the presynaptic marker Bassoon (Figure 2F), demonstrating that the mutated GluR1 has a normal synaptic localization in neuronal cultures similar to what was observed in vivo (Figure 2D). Taken together, these results suggest that the lack of GluR1 phosphorylation does not alter brain gross anatomy or the AMPA receptor distribution. Moreover, the GluR1 subunit lacking phosphorylation sites is properly targeted to synapses, indicating that the phosphorylation sites may not be critical for maintaining the steady-state level of receptors at synapses.

Deficient Synaptic Plasticity in the Phosphorylation Site Mutant Mice

Next, we looked at whether the lack of phosphorylation sites on GluR1 affects LTD and LTP expression in adult mice (3 months). All the electrophysiology experiments were done in a blind manner with littermate wild-type and homozygotes. To examine LTD, we used paired pulses at an interstimulus interval of 50 ms repeated at 1 Hz for 15 min (PP-1Hz), which has been previously used to induce LTD in hippocampal slices from adult rats (Kemp et al., 2000). The PP-1Hz protocol in the wild-type mice produced significant LTD (74% $\pm$ 4% of baseline measured at 1 hr from the onset of PP-1 Hz, n = 13 slices, seven mice; Figure 3A). In contrast, LTD was essentially abolished in the homozygous double phosphomutant littermates (96% $\pm$ 5% at 1 hr from the onset of PP-1Hz, n = 13 slices, seven mice; Figure 3A). In rats, this induction protocol has been reported to produce an NMDA receptor-dependent or mGluR-dependent LTD, depending on the age of the animal used (Kemp et al., 2000). We therefore tested whether LTD induction in mice using this protocol was sensitive to NMDA receptor antagonists. Bath application of 100 μM D,L-AP5, an NMDA receptor antagonist, completely blocked PP-1Hz-induced LTD in wild-type mice (105% $\pm$ 8% at 1 hr from the onset of PP-1Hz, n = 13 slices, six mice; Figure 3B).

In the adult homozygotes, LTP induced by a theta burst stimulation (TBS) was greatly reduced, albeit not completely absent, when compared to the wild-type littermates (−/−, 122% $\pm$ 10% measured 2 hr post TBS, n = 12 slices, seven mice; Wt, 176% $\pm$ 10% at 2 hr post TBS, n = 14 slices, seven mice; t test, $p < 0.005$; Figure 3C). To further confirm that the deficit in LTP is due to expression mechanisms and is not due to alterations in network activity or synaptic drive, we looked at pairing-induced LTP using intracellular sharp electrodes. When LTP was induced by pairing depolarizing current injection (+1 to +3 nA) with low-frequency stimulation (2 Hz, 100 pulses), the magnitude of pairing-induced LTP was severely reduced in the homozygotes (105% $\pm$ 6% of baseline at 45 min post pairing, n = 12 cells from ten mice) compared to the wild-type littermates (137% $\pm$ 12% of baseline at 45 min post pairing, n = 17 cells from 11 mice; t test, $p < 0.01$; Figure 3D). These results suggest that GluR1 phosphorylation plays a critical role in the expression of LTD and LTP.

A previous study has reported that deletion of the complete GluR1 gene eliminates LTP in adult mice but has little effect on LTP in young mice (1 month old), suggesting that there are GluR1-dependent and -independent forms of LTP that are developmentally regulated (Mack et al., 2001). We therefore examined whether the deficit in LTP in the double phosphomutant mice depended on age. Similar to the complete GluR1 knockouts, the LTP magnitude was normal in the young double phosphomutant mice (P21–P28; −/−, 129% $\pm$ 6% at 90 min post TBS, n = eight slices from five mice; Wt, 127% $\pm$ 11% at 90 min post TBS, n = 9 slices from five mice; t test, $p > 0.1$; Figure 3E). Interestingly, we found that LTD induced by a conventional 1 Hz (15 min) protocol was absent in the young (P21–P28) double phosphomutants (97% $\pm$ 3% at 1 hr post onset of 1 Hz, n = 13 slices, seven mice) when compared to wild-type littermates (80% $\pm$ 4% at 1 hr post onset of 1 Hz, n = 14 slices, seven mice; t test, $p < 0.01$; Figure 3F).

We wanted to confirm that the lack of LTD and the LTP deficit in the adult double phosphomutant mice were not due to nonspecific effects on synaptic transmission. First, we looked at basal synaptic transmission mediated by AMPA receptors by generating an input-output curve by measuring extracellular field potential responses with varying stimulus intensity. To control for the differential recruitment of presynaptic axons in different slices, we plotted the synaptic responses

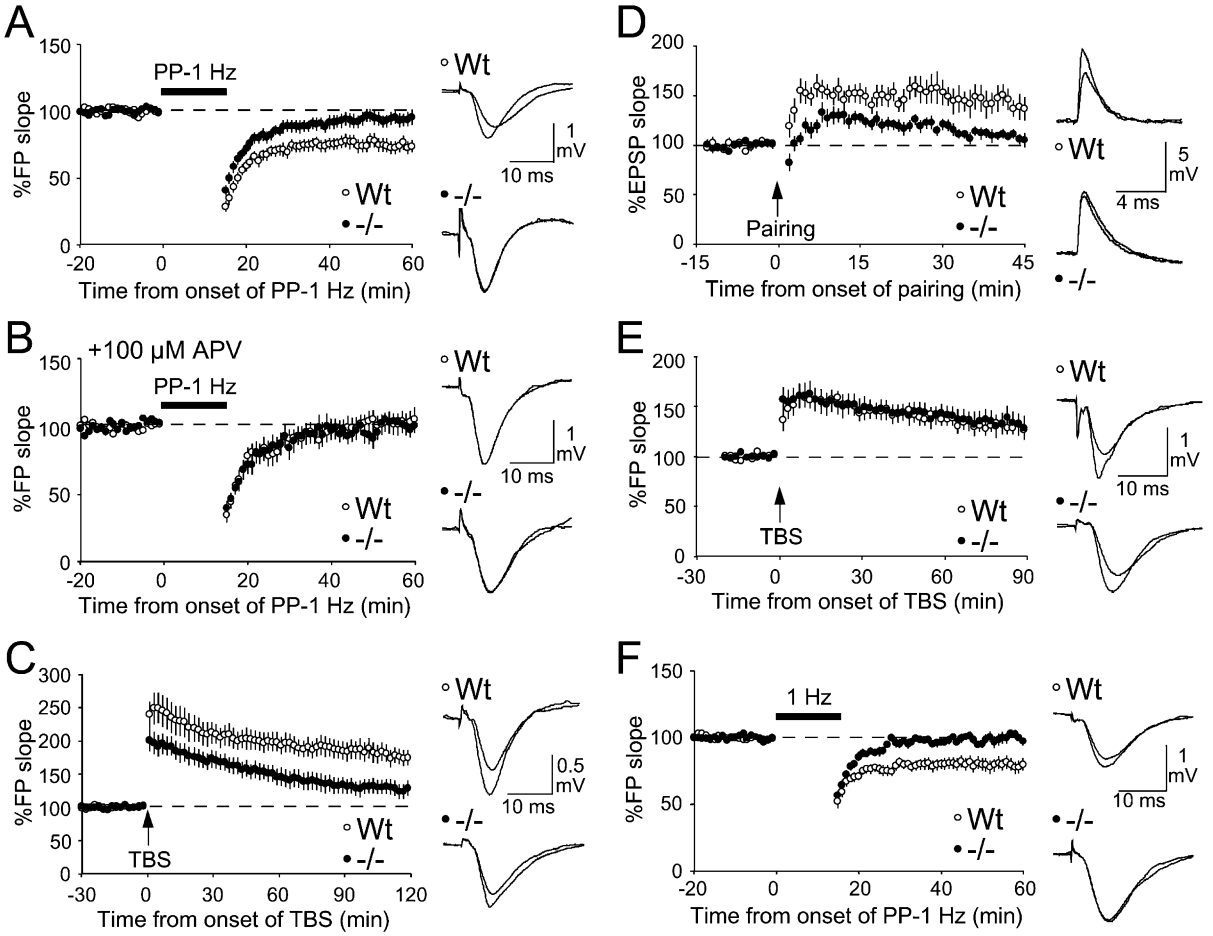

Figure 3. Lack of NMDA Receptor-Dependent LTD and Reduced LTP in the Double Phosphomutant Mice

(A) LTD is essentially abolished in the homozygotes (−/−, closed circles) compared to wild-type (Wt, open circles). LTD was induced by delivering PP-1 Hz for 15 min.

(B) LTD induced by PP-1 Hz is NMDA receptor-dependent in wild-type mice (Wt, open circles). Note that in homozygotes (−/−, closed circles), PP-1 Hz does not produce LTD with (B) or without (A) APV.

(C) LTP induced with theta burst stimulation (TBS) is reduced in the homozygotes (−/−, closed circles) compared to the wild-type littermates (Wt, open circles).

(D) Pairing induced LTP is also reduced in the homozygotes (−/−, closed circles) compared to wild-types (Wt, open circles). Recordings were done using intracellular sharp electrodes. LTP was induced by pairing depolarizing current injection (+1 to +3 nA), while giving 2 Hz (100 pulses) stimulation.

(E) LTP in young double phosphomutants is normal (−/−, closed circles; Wt, open circles). LTP was induced by TBS stimulation.

(F) Young double phosphomutants also lack LTD (−/−, closed circles; Wt, open circles). LTD was induced by delivering 1 Hz for 15 min.

An overlay of representative FP or EPSP traces taken during baseline and at the last few minutes of the recording are shown on the right side of each panel. Each trace is an average of four consecutive traces.

against presynaptic fiber volley amplitude (Figure 4A). We find that the input-output curves from homozygous and wild-type littermates are essentially identical, indicating that there are no obvious changes in basal synaptic strength. In order to test any possible alterations in presynaptic function, we measured paired-pulse facilitation (PPF) across different interstimulus intervals (ISIs) and found no differences in homozygotes compared to the wild-type littermates (Figure 4B). Since PPF is a sensitive measure of changes in presynaptic release probability, this indicates that presynaptic release function is normal in the double phosphomutants. Next, we tested whether the deficits in LTP and LTD were due to alterations in NMDA receptor-mediated synaptic transmission. We pharmacologically isolated NMDA receptor-mediated synaptic responses and normalized them to the fiber volley amplitude. We found that there were no differences in the NMDA receptor-mediated synaptic responses in the homozygotes compared to the wild-type littermates at all stimulation intensities measured (Figure 4C). In addition, we measured the ratio of AMPA to NMDA receptor-mediated synaptic currents in a whole-cell recording configuration and found no statistical difference (Wt, 1.7 ± 0.2, n = 26 cells; −/−, 2.1 ± 0.3, n = 28 cells; Student's t test, $p > 0.2$; Figure 4D). This attests that the mutations do not affect NMDA receptor-mediated synaptic responses. To further explore any potential changes in basal synaptic transmission, we measured AMPA receptor-mediated miniature excitatory postsynaptic currents (mEPSCs). We found that there are no significant differences in either the average amplitude or frequency of mEPSCs (amplitude, Wt =

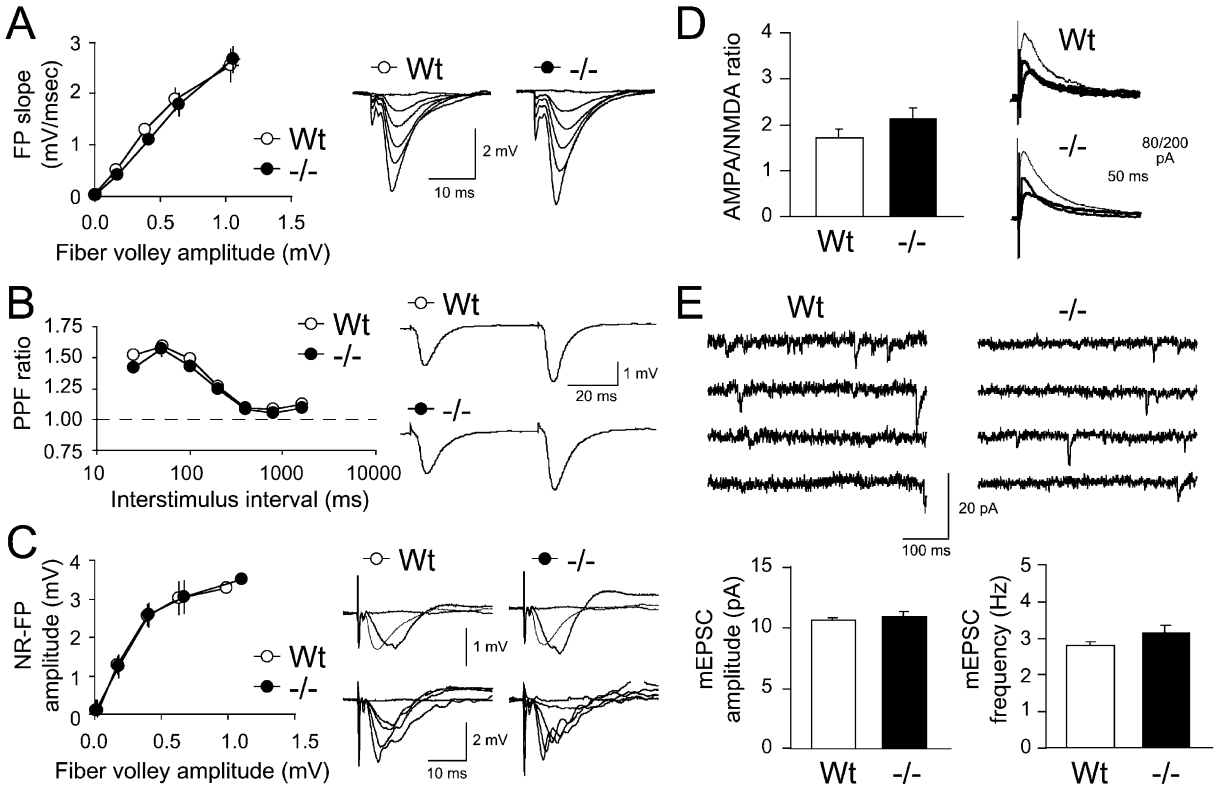

Figure 4. Normal Basal Synaptic Transmission and NMDA Receptor-Mediated Synaptic Responses in the Double Phosphomutant Mice

(A) Normal basal synaptic transmission measured as input-output function in homozygotes (−/−, closed circles) compared to wild-types (Wt, open circles). To correct for the variability in recruitment of presynaptic fibers, we plotted FP slopes against presynaptic fiber volley amplitudes. Representative traces (averages of three consecutive FPs elicited with the same stimulation intensity) are shown on the right. Average traces from varying intensities are overlapped for wild-type (Wt) and homozygote (−/−).

(B) No differences in paired-pulse facilitation (PPF) ratio between wild-type (Wt, open circles) and homozygotes (−/−, closed circles). Representative examples from wild-type (Wt) and homozygote (−/−) at 50 ms ISI are shown on the right.

(C) Pharmacologically isolated NMDA receptor-mediated responses in wild-type (Wt, open circles) and homozygotes (−/−, closed circles). There is no difference between wild-type and homozygotes when plotting NMDA receptor-mediated responses against fiber volley amplitude. Representative traces are shown to the right. Thin traces are normal FP responses, mainly mediated by AMPA receptors. Thick traces are pharmacologically isolated NMDA receptor-mediated FPs, which have a slower latency. Gray thick traces are NMDA receptor mediated FPs after the addition of 100 μM APV. Note that there are no synaptic responses while the fiber volley remains intact.

(D) NMDA/AMPA current ratio measured in whole-cell does not differ between wild-types and mutants. Measurements shown in the figure were collected at a holding potential of +28mV, but we also saw no change in NMDA/AMPA ratio measured at −40mV (data not shown). There was no noticeable rectification of AMPA receptor-mediated currents in either wild-type or mutants (data not shown). Example traces are shown on the right. Thin solid lines, total currents; thick solid lines, isolated NMDA receptor-mediated currents; thick gray lines, subtracted AMPA receptor-mediated currents.

(E) No difference in AMPA receptor-mediated mEPSC amplitude or frequency between wild-types and mutants. Pharmacologically isolated AMPA mEPSCs were measured at holding potential of −68mV. Example mini traces are shown on the top for each genotype.

10.7 ± 0.2 pA, −/− = 11.0 ± 0.3 pA; frequency: Wt = 2.8 ± 0.1 Hz, n = 9; −/− = 3.2 ± 0.2 Hz, n = 16; Figure 4E). Collectively, these results suggest that the deficits in LTP and LTD are not due to abnormalities in synaptic transmission or NMDA receptor-mediated synaptic responses but are likely due to the lack of LTP- and LTD-induced changes in GluR1 phosphorylation and the absence of the resulting modification of receptor function.

Deficient Dynamic Membrane Trafficking of AMPA Receptors in the Phosphorylation Site Mutant Mice

Phosphorylation of GluR1 on S831 and S845 has been shown to potentiate AMPA receptor channel function (Banke et al., 2000; Barria et al., 1997a; Derkach et al., 1999; Roche et al., 1996), suggesting that the lack of LTP- and LTD-induced phosphorylation and dephosphorylation of these sites and the lack of the subsequent changes in channel function may mediate the deficits in LTP and LTD. However, previous studies have provided evidence that the rapid membrane insertion or internalization of AMPA receptors is critical for LTP and LTD expression (Carroll et al., 2001; Luscher and Frerking, 2001). To further address the potential mechanism of the deficits in synaptic plasticity, we looked at the membrane trafficking of AMPA receptors in neuronal cultures generated from wild-type and homozygous mice. We hypothesized that the deficits in LTP and LTD in the GluR1 phosphorylation site mutant mice may be due to a defect in AMPA receptor membrane trafficking in addition to any effects on channel function. To look

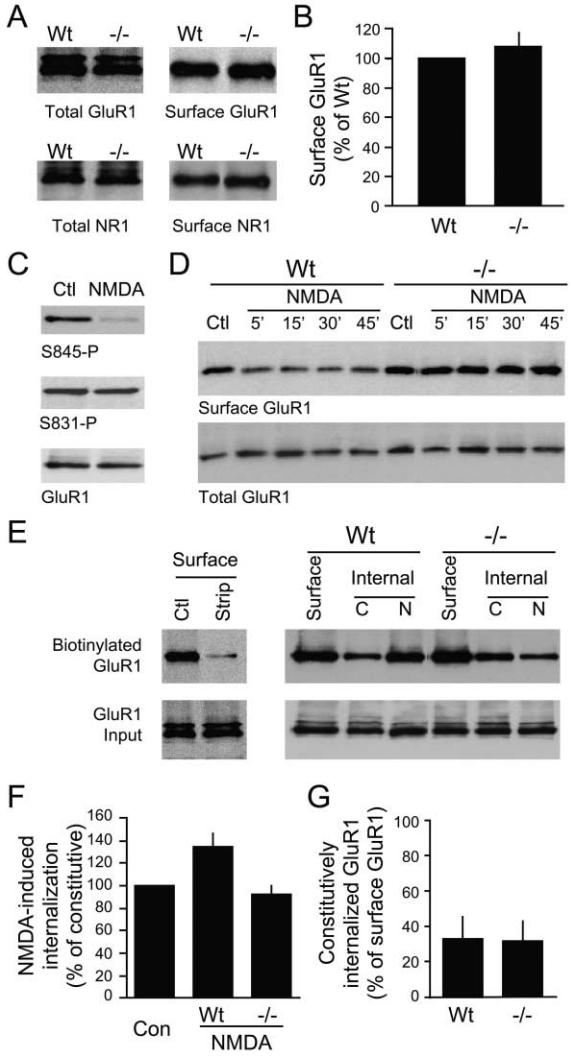

Figure 5. A Defect in NMDA-Induced Internalization of AMPA Receptors in Neuronal Culture from GluR1 Double Phosphomutant Mice

(A) Normal surface expression of GluR1 in double phosphomutants. Cultured cortical neurons prepared from wild-type (Wt) and homozygotes (−/−) were used for steady-state biotinylation of surface GluR1 (top) and NR1 (bottom). Total GluR1 and total NR1 are shown to the left, and biotinylated surface GluR1 and NR1 are shown to the right.

(B) Quantification of surface GluR1. There was no significant difference in the steady-state surface expression of GluR1 between wild-types (Wt) and homozygotes (−/−).

(C) NMDA treatment dephosphorylated GluR1 on S845. Cortical cultured neurons from wild-type mice were treated with NMDA for 15 min. The control and NMDA-treated samples were probed with α-GluR1-S831 Ab or α-GluR1-S845 Ab. Note that there is a decrease in phospho-signal using α-GluR1-S845 Ab. The blots were stripped and reprobed with GluR1C Ab to measure total amount of GluR1 in each sample.

(D) NMDA treatment decreases surface GluR1 in wild-type mice (Wt), but not in homozygous mice (−/−). Cortical cultures prepared from wild-type, and homozygous mice were used for surface biotinylation. The blots were probed with α-GluR1C Ab. Top is the biotinylated samples that shows surface GluR1. Bottom shows the total GluR1 (input) for each sample. In wild-types, there was a decrease in surface GluR1 at 5, 15, 30, and 45 min treatment with NMDA. There was no decrease in surface GluR1 level in homozygotes after NMDA treatment.

(E) NMDA treatment increases internalization of GluR1 in wild-types (Wt), but not in homozygotes (−/−). Internalized surface GluR1 was measured using biotin-strip protocol using cortical cultures prepared from wild-type and homozygotes (see Experimental Procedures). Top shows that under control conditions, stripping removes biotin labeling of surface receptors. Inputs are shown at the bottom left. Biotinylated surface GluR1 measured without stripping in wild-type (lane 1) and homozygote cultures (lane 4). Internalization of surface GluR1 under control conditions, which is measured by biotinylating surface receptors and stripping after 15 min at 37 C in wild-type (lane 2) and homozygote (lane 5). Internalization of GluR1 after 15 min treatment with NMDA in wild-type (lane 3) and homozygote cultures (lane 6). Note an NMDA-induced increase in wild-type GluR1 internalization (compared to control internalization shown in lane 2), while there is no NMDA-induced increase in homozygotes GluR1 internalization (compared with lane 5). The bottom right panel shows the GluR1 input signal for the results shown in upper right panel.

(F) Quantification of NMDA-induced internalization between wild-type and phosphomutants. Internalized GluR1 after NMDA treatment (as shown in [E]) was quantified and normalized as a percentage of constitutive internalization. NMDA-induced increase in internalization of GluR1 in wild-type (Wt, n = 3) is not present in the phosphomutants (−/−, n = 3).

(G) Quantification of constitutive internalization of GluR1 from internalization assays described in [E]. Constitutively internalized GluR1 is expressed as a percentage of surface GluR1.

closely at the dynamics of the membrane localization of AMPA receptors, we performed surface biotinylation on the neuronal cultures. Steady-state surface biotinylation of the neurons showed equivalent levels of surface GluR1 in both wild-type and homozygous cultures (Figures 5A, 5B, and 5E), further indicating that the mutation of both phosphorylation sites does not affect the steady-state surface expression of GluR1. Recent studies have shown that NMDA treatment of slices or neuronal cultures induces an LTD-like synaptic depression, a selective dephosphorylation of S845 (Ehlers, 2000; Kameyama et al., 1998; Lee et al., 1998), and internalization of AMPA receptors (Beattie et al., 2000; Ehlers, 2000). This paradigm has served as a cell culture model for NMDA receptor-dependent LTD. We therefore examined whether NMDA-induced internalization of AMPA receptors was affected in the double phosphomutant mouse cultures. We confirmed that NMDA treatment induces a dramatic dephosphorylation of GluR1 on S845 (48% ± 5% of control, n = 5), with less dephosphorylation of S831 (69% ± 3% of control, n = 5) in wild-type mouse cultures (Figure 5C). To analyze for NMDA-induced changes in surface GluR1 expression, we treated neurons with or without NMDA for 15 min, placed the cells on ice to stop membrane trafficking, and used cell-surface biotinylation methods to isolate the cell surface GluR1. NMDA treatment of neurons rapidly decreased the surface levels of GluR1 in the wild-type mouse cultures but had little effect on surface GluR1 in the phosphomutant cultures (Figure 5D). To more specifically look at internalization of AMPA receptors, we first labeled the surface receptors with biotin and then allowed the receptors to internalize at 37 C in the presence or absence of NMDA. Then the surface biotin was "stripped" such that the only remaining biotin-labeled receptors were the ones that had undergone internalization. In neurons from wild-type mice, NMDA treatment for 15 min produced an internalization of GluR1 compared to control neurons without NMDA treatment (n =

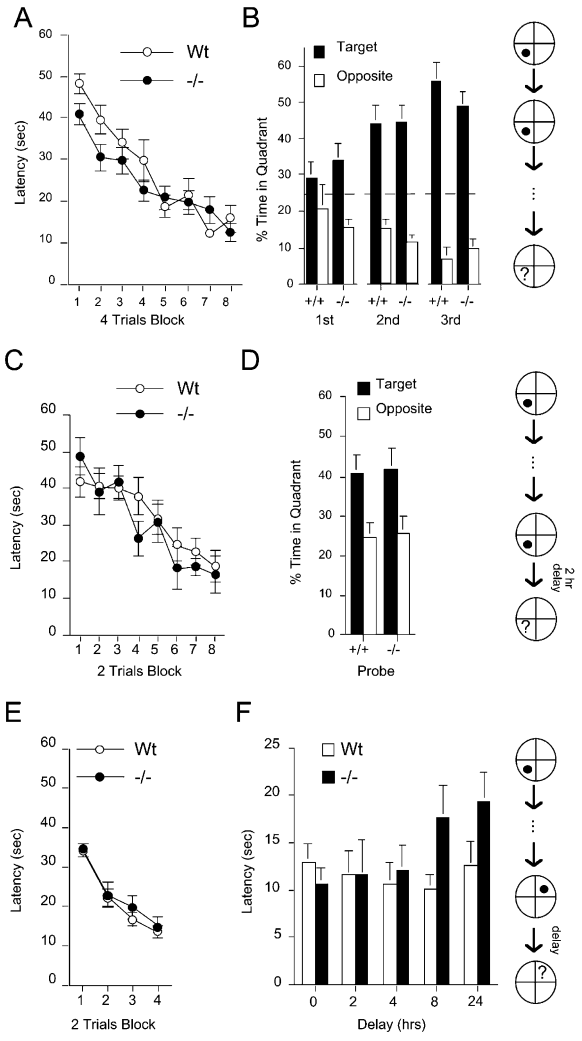

Figure 6. Double Phosphomutants Learn Normally but Show a Specific Impairment in Retention of Spatial Information in the Morris Water Maze

(A) Phosphomutants learn normally in Morris water maze. There was no difference between groups of male adult (>3 months old) wild-type (Wt) and homozygotes (−/−) in latency to find the hidden platform during the training trials.

(B) After the training trials, the hidden platform was removed after the fourth (first probe trial), sixth (second probe trial), and eighth (third probe trial) training trials to conduct a probe trial. Both wild-type (Wt) and homozygotes (−/−) gradually spent more time in the target quardrant searching for the platform, suggesting normal learning of the platform location.

(C) A new set of wild-type (n = 11) and homozygous (n = 9) male mice were initially trained with a fixed platform location. There was no difference in performance between the two groups.

(D) The animals were subsequently tested on retention using a probe trial given with a 2 hr delay after the training on the fixed platform location. Both wild-type and homozygotes spent more time in the target quadrant.

(E) After familiarization with the procedures, mice were trained with a novel platform location for each day's session and assessed with retention tests at varying delays. Both wild-type and homozygotes proficiently learned the escape platform location within each training session such that training trial performance did not differ between groups in any session of new learning.

(F) Retention tests revealed impairment in the mutant mice relative to wild-type mice at delays of 8 and 24 hr ($p < 0.05$, ANOVA), but not at shorter delays (0–4 hr). Additional analysis of the 8 and 24 hr delay sessions indicated that wild-type mice had excellent savings at these long delays because no difference was evident in comparing latencies on the last training trial and latencies in the retention tests. In contrast, mutant mice had significantly less savings as determined by comparing retention trial and training trial performance at both the 8 and 24 hr delays ($p < 0.02$). There was no difference in the swim speed between wild-type and mutants (Wt, 23.4–33.8 cm/s; −/−, 23.8–34.1 cm/s). Schematic drawings of the behavioral tasks are shown on the right hand side of each panel.

3, Figures 5E and 5F). In contrast, in the double phosphomutant mouse cultures, the NMDA treatment did not induce internalization of GluR1 compared to control neurons (n = 3; Figures 5E and 5F). Despite the differences in NMDA-induced internalization, constitutive internalization under basal conditions was similar in wild-type and homozygotes (Figure 5G). Collectively, these results demonstrate that NMDA-induced internalization of AMPA receptors containing the GluR1 subunit is inhibited in the double phosphomutant mice.

Deficient Retention of Spatial Memory in the Phosphorylation Site Mutant Mice

Since we saw profound deficits in LTD and LTP in the hippocampal CA1 region, we wanted to test the mice for hippocampal-dependent spatial cognition. First, we tested the double phosphomutants in the standard Morris water maze task with a hidden platform. The performance of both wild-types and double phosphomutant mice in escaping to the hidden platform improved during the training trials, as measured by reduced escape latencies (Figure 6A). To test whether the animals indeed learned the spatial location of the hidden platform, we ran probe trials in which the platform was removed. To our surprise, both the wild-type and homozygous mice gradually spent more time in the target quadrant searching for the platform, suggesting that they both learned the location of the hidden platform (Figure 6B). Since the phosphomutants showed normal learning in the standard water maze task, we next wanted to determine if they had deficits in tests of rapidly acquired spatial memory. To analyze this, a new cohort of mice was trained for two days in the water maze with a fixed platform location (Figures 6C and 6D). Both wild-type and homozygotes performed equally in the training sessions (Figure 6C), using probe trials with 2 hr delays (Figure 6D), consistent with normal learning seen in the previous experiments (Figures 6A and 6B). The mice were then trained each subsequent day to escape to a new platform location, and retention tests were given at varying delays after each episode of new learning (Figures 6E and 6F). Within each training session, the performance of the wild-type and homozygous mice did not differ (Figure 6E), again suggesting normal learning of the task. However, the mutant mice had a selective impairment in the retention of new learning at delays longer than a few hours. The phosphomutant mice could remember the new location after short delays (2–4 hr) but had poor retention at 8 or 24 hr after an episode of new learning (Figure 6F).

Discussion

GluR1 Phosphorylation, Synaptic Plasticity, and Memory

In this study, we identify a key protein kinase and phosphatase substrate that mediates the expression of synaptic plasticity. Specifically, we demonstrate that mice lacking phosphorylation sites on the GluR1 subunit of AMPA receptors show deficits in synaptic plasticity and retention of spatial memory. The GluR1 phosphorylation site mutant mice essentially lack NMDA receptor-dependent LTD and show reduced LTP compared to wild-type littermates. This indicates that the phosphorylation of the AMPA receptor GluR1 subunit is critical for LTD expression and is important for the stability of LTP. Phosphorylation and dephosphorylation of S831 and S845 of GluR1 have been shown to modulate AMPA receptor ion channel properties (Banke et al., 2000; Derkach et al., 1999; Roche et al., 1996). Phosphorylation of S831 increases the apparent single-channel conductance, while phosphorylation of S845 increases the apparent open-channel probability of AMPA receptors. Mutation of the phosphorylation sites prohibits modulation of the phosphorylation state and ion channel properties of the receptor during LTP and LTD and, thus, inhibits synaptic plasticity. This is consistent with a previous study that reported changes in the ion channel conductance of AMPA receptors after LTP induction (Benke et al., 1998).

Recent studies have suggested that the level of AMPA receptors at synapses are also modulated during LTP and LTD (Song and Huganir, 2002). LTP expression has been proposed to be dependent on the rapid synaptic insertion of GluR1 subunit-containing receptors (Hayashi et al., 2000; Shi et al., 2001), and several groups have provided evidence that endocytosis of AMPA receptors is important for LTD expression (Beattie et al., 2000; Carroll et al., 1999; Ehlers, 2000; Man et al., 2000). Although the insertion of GluR1-containing AMPA receptors appears to be independent of phosphorylation of the S831 site (Hayashi et al., 2000), S845 phosphorylation has recently been suggested to be important (Esteban et al., 2003). Moreover, the internalization and recycling of AMPA receptors has been correlated with changes in S845 phosphorylation (Ehlers, 2000). Interestingly, NMDA-induced internalization of AMPA receptors is inhibited in the phosphomutant mice, suggesting that dephosphorylation of S845, in addition to its effects on the open-channel probability of the receptor, may regulate the stability of the receptor on the surface and thus regulate NMDA-induced internalization. Taken together with our previous result that LTD is correlated with a dephosphorylation of GluR1 S845 (Kameyama et al., 1998; Lee et al., 2000; Lee et al., 1998), our present finding strongly indicates that LTD-induced internalization of AMPA receptors is regulated by S845 phosphorylation. Phosphorylation of S845 may stabilize the GluR1 in the plasma membrane, and dephosphorylation allows the dynamic regulation of receptor internalization. This stabilization of surface GluR1 by phosphorylation may also play a role in the stability of LTP. LTP-inducing stimuli may promote AMPA receptor insertion in a manner that is regulated by S845 phosphorylation (Esteban et al., 2003), but our data also suggest that S845 phosphorylation inhibits internalization of the newly inserted receptors, stabilizing LTP.

Previous reports showed that LTP is essentially absent in adult GluR1 knockout mice (Mack et al., 2001; Zamanillo et al., 1999). Our finding that LTP is not completely absent in the double phosphomutants suggests that there are at least two components to LTP expression in adult mice: a GluR1 phosphorylation-dependent and a GluR1 phosphorylation-independent component. In addition, our results are consistent with results showing normal LTP in young GluR1 knockout mice (Mack et al., 2001), supporting the idea that there are developmentally regulated GluR1-dependent and -independent forms of LTP. In contrast, we find that LTD in both young and adult animals depends on GluR1 phosphorylation, suggesting a conserved mechanism for LTD expression during development.

In spite of the key role of GluR1 phosphorylation in hippocampal LTD demonstrated here, several lines of evidence have suggested that the GluR2 subunit also plays a critical role in AMPA receptor internalization during LTD (Daw et al., 2000; Kim et al., 2001; Man et al., 2000). Intracellular perfusion of synthetic peptides that disrupt the interaction of the GluR2 subunit with PDZ domain-containing scaffolding proteins inhibits LTD expression, indicating that these interactions may be important for the internalization of AMPA receptors during LTD (Chung et al., 2000; Daw et al., 2000; Kim et al., 2001; Matsuda et al., 1999). Our observation that mutation of GluR1 phosphorylation abolishes LTD indicates that the GluR1 phosphorylation may interact with GluR2-dependent mechanisms of LTD.

A working model of the role of GluR1 phosphorylation in LTP and LTD is illustrated in Figure 7. In the wild-type mice, high-frequency stimulation (HFS) used for LTP induction promotes the phosphorylation and insertion of GluR1-containing AMPA receptors into synapses. The phosphorylation-induced potentiation of receptor ion channel properties and the increased levels of synaptic receptors are both important for potentiating synaptic transmission. The synaptic insertion process may be regulated by S845 phosphorylation (Esteban et al., 2003), but S831 phosphorylation does not appear to be necessary (Hayashi et al., 2000). In addition, our data indicates that phosphorylation of GluR1 stabilizes the synaptic receptors and thus stabilizes LTP (Figure 7A, top). Alternatively, GluR1 phosphorylation may act as a "tag" to allow replacement of GluR1/GluR2 receptors by GluR3-containing receptors as proposed previously (Shi et al., 2001). In contrast, in the phosphomutant mice (Figure 7A, bottom), the mutated phosphorylation sites prevent the HFS-induced GluR1 phosphorylation and the resulting potentiation of receptor ion channel properties, the regulation of receptor delivery, and the stabilization of surface receptors after the initial insertion. On the other hand, LTD induction by low-frequency stimulation (LFS) in wild-type mice induces dephosphorylation of synaptic AMPA receptors on GluR1 subunits, which inhibits the ion channel properties of the receptor and decreases the plasma membrane stability of the receptors. This dephosphorylation is essential for the activity-dependent internalization of AMPA receptors (Figure 7B, top). In contrast, the lack of phosphorylation sites on GluR1 in the mutant mice prevents the LFS-induced

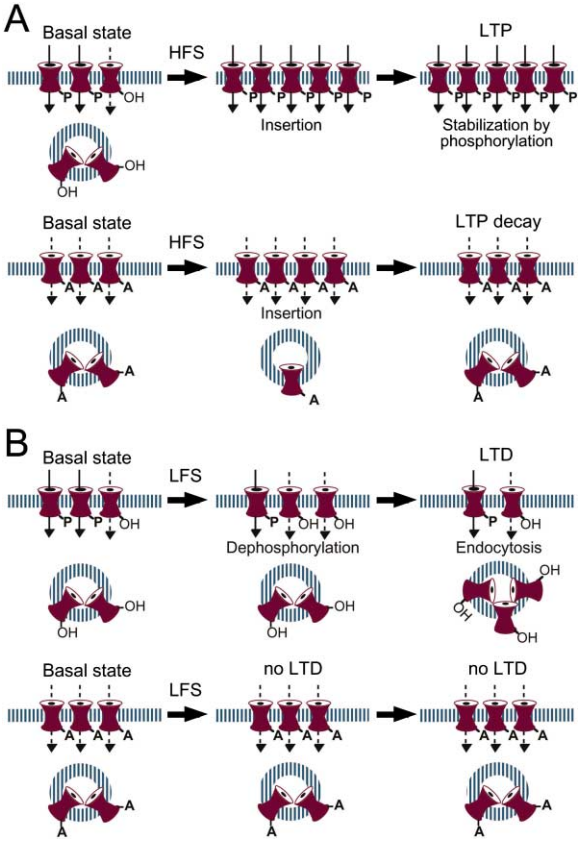

Figure 7. Model of the Role of GluR1 Phosphorylation in LTP and LTD Expression

(A) Top, wild-types. Upon LTP induction by high-frequency stimulation (HFS), GluR1-containing AMPA receptors are inserted into the synaptic membrane. Phosphorylation of GluR1 may regulate the insertion; however, it is not necessary for the insertion. The inserted receptors require phosphorylation of GluR1 subunit to stay at the synapse. Alternatively, phosphorylation of GluR1 may act as a "tag" to signal replacement by GluR2-containing receptors, as previously proposed (Shi et al., 2001). Bottom, double phosphomutants. HFS inserts the mutant AMPA receptors; however, the lack of phosphorylation sites prevents these receptors from staying at the synapse or getting replaced by GluR2-containing receptors. Therefore, the LTP is not stable over time.

(B) Top, wild-types. Upon LTD induction by low-frequency stimulation (LFS), GluR1 subunits are dephosphorylated, which leads to endocytosis. Bottom, double phosphomutants. Activity-induced internalization of the receptors by LFS is not present in the mutants.

changes in GluR1 phosphorylation and the dynamic regulation of receptor channel properties and internalization (Figure 7B, bottom).

This model does not adequately explain why the basal levels of synaptic GluR1, AMPA receptor-mediated synaptic transmission, and constitutive GluR1 endocytosis are normal in the phosphomutants. According to the model, the lack of phosphorylation would decrease the levels of synaptic receptors and the AMPA receptor-mediated synaptic transmission by decreasing the surface stability and ion channel properties of the receptor. In addition, the lack of phosphorylation would enhance the constitutive GluR1 internalization. However, it is likely that compensatory homeostatic mechanisms modulate the steady-state function of AMPA receptors to maintain proper levels of neuronal excitability. It is clear, however, that GluR1 phosphorylation is critical for the dynamic regulation of AMPA receptor function during LTP and LTD.

The GluR1 phosphorylation sites are not only critical for synaptic plasticity, but also appear to be important for spatial memory. Using water maze tests, we find that the learning of spatial tasks is intact in the double phosphomutant mice. This is in accordance with the reported normal spatial learning of GluR1 knockout mice (Zamanillo et al., 1999; Reisel et al., 2002). However, we find that the retention of rapidly acquired new learning is impaired in the GluR1 double phosphomutants. In such settings, the mutant mice were able to learn as well as the wild-type mice but did not retain this memory after 8–24 hr. This is interesting considering the instability of the LTP in the GluR1 phosphomutants and suggests that this rapidly decaying LTP may not allow for consolidation of the memories beyond 4 hr in this task. Our test for rapidly acquired episodes of new spatial learning is similar to episodic or working memory tests used in recent studies (Zheng et al. 2001; Reisel et al. 2002). It has been proposed that NMDA receptor-dependent hippocampal LTP is important for one-trial learning episodic memory rather than multitrial spatial reference memory (for example, the fixed platform water maze test we have used in our study) (Morris and Frey, 1997). One caveat to the interpretation of our results is that similar to most behavioral experiments with knockout or knockin mice, we are using a hybrid genetic background that may complicate the behavioral analysis. It is interesting to note, however, that a recent study reported that GluR1 knockouts have a selective deficit in a spatial working memory task despite having normal performance in reference memory tasks (Reisel et al., 2002). Taken together with our results, this indicates that GluR1-dependent LTP in adult CA1 may be important for rapidly learned episodic spatial memory, and phosphorylation of GluR1 may be necessary for the retention of such memory.

This study demonstrates that the phosphorylation of two sites on the AMPA receptor GluR1 subunit is critical for the expression and maintenance of NMDA receptor-dependent LTP and LTD and for the retention of spatial learning tasks. LTP and LTD are implicated not only in memory formation, but also in other diverse brain functions such as fine tuning of synaptic connections during development and rewiring of connections after brain injury (Buonomano and Merzenich, 1998), motor skill learning (Lisberger, 1998; Sanes and Donoghue, 2000), and drug addiction (Hyman and Malenka, 2001). Since the basic cellular mechanisms of NMDA receptor-dependent LTP and LTD are quite conserved across different brain regions, our results from the hippocampus of GluR1 double phosphomutants is likely applicable to other brain areas. It is known that phosphorylation of GluR1 is regulated by many factors including activation of dopamine receptors (Price et al., 1999; Snyder et al., 2000) and -adrenergic receptors (H.-K.L., R.L.H., and A.K., unpublished data), and by psychoactive drugs such as cocaine, methamphetamine, and fluoxetine (Prozac) (Snyder et al., 2000; Svenningsson et al., 2002). Therefore, these mice will also be useful for the analysis of the role of these modulatory events on AMPA receptor and brain function.

Experimental Procedures

Generation of Mice Lacking Phosphorylation Sites on GluR1

To construct the targeting vector, a 10.5 kb Nhe I-Spe I fragment containing exon 17 of GluR1 was isolated from 129/Svj mouse genomic BAC library (Incyte Genomics). The targeting vector was comprised of a 2.5 kb short arm and 8.0 kb long arm with PGK-*neo* flanked by two lox-P sites and the thymidine kinase gene (MC1-tk). The 3 -side long arm contained exon 17 with the two phosphorylation sites, serines 831 and 845, mutated to alanine. In addition, a silent Sac II site mutation was introduced between the alanine mutation sites to distinguish mutant allele from wild-type. All mutation procedures were carried out by site directed PCR mutagenesis (Stratagene). The targeting construct was electroporated into R1 ES cells (129/Sv 129/Sv-CP F1) (Nagy et al., 1993). Positive clones were identified by polymerase chain reaction (PCR) and confirmed by Southern blot using an outer probe (probe A in Figure 1A). Four positive ES clones were injected into C57BL/6 blastocysts, and chimeras were crossed to C57BL/6 mice. These mice were crossed to CMV-*Cre* (129 and C57BL/6 hybrid genetic background) to remove the *neo* cassette from the germ line through *cre*/*loxp*-mediated excision (Nagy et al., 1998). After confirmation of *neo*^{r} excision by PCR and Southern blot analysis, heterozygous mice were bred to produce homozygotes, and mutants in which the *cre* gene was absent were used for subsequent breeding. The intercross of heterozygotes resulted in production of wild-type, heterozygous, and homozygous offspring at the expected 1:2:1 Mendelian ratio. For all analyses, mice with 129 and C57BL/6 hybrid genetic background were used. All procedure relating to animal care and treatment conformed to the institutional and NIH guidelines.

Immunoblots

Brains dissected from wild-type, heterozygous, and homozygous mice were quickly frozen in liquid nitrogen. The samples were homogenized in ice-cold lysis buffer (20 mM $NaPO_4$, 300 mM NaCl, 10 mM EDTA, 10 mM EGTA, 10 mM sodium pyrophosphate, 50 mM NaF, 1 mM Na_3VO_4, 1 μM okadaic acid, and 10 U/ml aprotinin), and crude membranes prepared as previously described (Lee et al., 2000). The primary antibodies (Abs) were diluted in blocking buffer (1% bovine serum albumin and 0.1% Tween-20 in PBS). The blots were developed using either enhanced chemifluorescence (ECF, Amersham) or enhanced chemiluminescence (ECL, NEN). For ECF, secondary Ab linked to alkaline phosphatase was used, and for ECL, secondary Ab linked to horseradish peroxidase was used. ECF blots were scanned using a Storm860 scanner (Molecular Dynamics), while ECL blots were exposed to BioMax film (Kodak) and scanned using a Personal Densitometer (Molecular Dynamics). Blots were quantified using ImageQuant™ software (Molecular Dynamics).

Histology and Immunohistochemistry

The brains were perfused and fixed in 4% paraformaldehyde and transferred to a 30% sucrose solution. Coronal sections were cut at 40 μm thickness and collected into cold 0.1 M phosphate buffered saline. Sections were stained with cresyl violet and observed under the light microscope or processed for immunohistochemistry using anti-GluR1 C-terminal Ab or anti-GluR2 C-terminal Ab.

Immunogold Electron Microscopy

For immuno-electron microscopy, the hippocampi of wild-type and mutant mice were processed for postembedding immunogold labeling, as described previously (Petralia et al., 1999; Petralia and Wenthold, 1999). Briefly, animals were anesthetized and perfused, and brains were sectioned, frozen in liquid propane in a Leica CPC (Vienna, Austria), freeze-substituted in a Leica AFS, and immunolabeled (10 nm gold).

Immunostaining of Cultured Hippocampal Neurons

Wild-type or homozygous P1 mice hippocampi were dissociated by trypsin and then subsequently plated onto coverslips coated with a confluent glial feeder layer. Each set of mice was dissected on the same day under the same culturing conditions. Staining was performed on DIV14. Briefly, neurons were labeled live with GluR1 N-terminal Ab (GluR1-N), and the tissue was then fixed and permeabilized followed by addition of Bassoon monoclonal Ab (Stressgen). FITC and Cy3 conjugated secondary Abs were added to visualize fluorescent signals.

Electrophysiology

Hippocampal slices (400 μm thick) were prepared from adult male mice as described previously (Lee et al., 2000). In brief, hippocampi were dissected using ice-cold dissection buffer (212.7 mM sucrose, 2.6 mM KCl, 1.23 mM NaH_2PO_4, 26 mM $NaHCO_3$, 10 mM dextrose, 3 mM $MgCl_2$, and 1 mM $CaCl_2$), and recovered at room temperature in ACSF (124 mM NaCl, 5 mM KCl, 1.25 mM NaH_2PO_4, 26 mM $NaHCO_3$, 10 mM dextrose, 1.5 mM $MgCl_2$, and 2.5 mM $CaCl_2$). All recordings were done in a submersion recording chamber perfused with ACSF (29 C–30 C, 2 ml/min). Synaptic responses were digitized and stored online using Igor software (Wavemetrics). LTP was induced using a theta burst stimulation (TBS: four trains, each consisting of ten 100 Hz bursts [four pulses] given at 5 Hz, repeated at 10 s intervals). LTD was elicited using a paired-pulse 1 Hz protocol (PP-1Hz: paired-pulses of 50 ms interstimulus interval (ISI) repeated at 1 Hz for 15 min). For measurement of paired-pulse facilitation (PPF), we used ISIs of 25, 50, 100, 200, 400, 800, and 1600 ms. Pharmacologically isolated NMDA receptor-mediated synaptic responses were measured using 0 mM $MgCl_2$ ACSF with 10 μM NBQX. 100 μM APV was added at the end of each experiment to confirm the NMDA receptor-mediated response. Intracellular recordings were done using sharp electrodes (tip resistance: 80–150 MΩ) filled with 3 M K-acetate and 10 mM KCl. Cells were held at around −70mV by manual current injection. Pairing LTP was elicited by pairing depolarizing current injection (+1 to +3 nA to bring membrane potential close to 0mV) and 2 Hz (100 pulses) afferent stimulation.

Whole-Cell Recording

For AMPAR-mediated mEPSC measurement, 1 μM tetrodotxin (TTX), 100 μM DL-2-amino-5-phosphonovaleric acid (APV), 100 μM picrotoxin, and 10 μM bicuculline were added in bath ACSF (124 mM NaCl, 2.5 mM KCl, 1.25 mM NaH_2PO_4, 26 mM $NaHCO_3$, 10 mM dextrose, 1.3 mM $MgCl_2$, 2.5 mM $CaCl_2$). The cells were held at −68mV, and recordings were done at 32 C. Continuous 500 ms traces were collected at 3 s interval and filtered at 2 kHz. Cells with series resistance 13 MΩ were discarded.

For AMPAR-EPSC/NMDAR-EPSC peak amplitude ratio measurements, cells were held initially at −68mV to collect baseline EPSC responses for 6–8 s. After stable baseline, holding potential was changed to 0mV to check the voltage clamp, then further changed to +25mV. After collecting 20–40 sweeps, ACSF was switched to one containing the AMPAR antagonist 10 μM 2,3-dioxo-6-nitro-1,2,3,4-tetrahydrobenzo[f]quinoxaline-7-sulfonamide (NBQX) and another 50–80 sweeps were collected. To get pure AMPAR-mediated EPSC component, subtraction between ten average responses ±NBQX was done. From these pure AMPAR- and NMDAR-mediated average EPSCs, the ratio of the peak amplitude of AMPAR- and NMDAR-mediated EPSC was made. Only one cell was recorded from each slice to avoid the incomplete washout of NBQX.

Biotinylation and Internalization Assay in Neuronal Cultures

2.5- to 3-week-old mouse cortical neurons cultured in 6 cm dishes were used. Surface biotinylation and receptor internalization analysis were performed using protocols described previously with minor modifications (Ehlers, 2000; Mammen et al., 1997). Briefly, neurons were pretreated with 100 μM NMDA for different periods of time, then incubated with 1 mg/ml sulfo-NHS-S-S-biotin (Pierce) in ACSF for 25 min at 10 C. The biotinylated cell-surface proteins were precipitated following incubation of the cell lysates with UltraLink immobilized neutravidin beads (Pierce). For receptor internalization assay, cells were surface biotinylated, rinsed with ACSF (the same as used for whole-cell recording), and transferred to 37 C with or without NMDA treatment (100 μM, 15 min). The remaining surface biotinylation was stripped using reduced glutathione, and the internalized receptors protected from stripping were then isolated and analyzed using immunoblots. Phosphospecific Abs against GluR1 S845 and S831 were used to determine the NMDA effects on GluR1 phosphorylation.

Behavioral Analysis

All mice used were 3- to 4-month-old male F4 129 C57BL/6 hybrid, obtained by mating heterozygous F3. Mice were trained in a 1.5 m diameter water maze (opaque water at 27 C with 12 cm diameter escape platform at 0.38 cm below water surface, 10 min intertrial interval, maximum trial duration of 60 s with 20 s on the platform at the end of each trial). First, nine wild-type and ten homozygous male mice received four trials/day for 8 days with probe trials (30 s duration) given 24 hr after the fourth, sixth, and eighth training sessions and 5 days after completion of the training protocol. In a second set of experiments, a new set of mice received 2 days of initial training (eight trials each) with a fixed platform location followed by a 30 s probe trial at a 2 hr delay. In each session for the next 11 days, mice were trained (eight trials) to locate the platform at a novel location in each daily session. For the first 4 days, mice were acclimated to this task with retention tests given either immediately or 2 hr after training. For subsequent experimental sessions, the retention trials were conducted at delays of 0, 2, 4, 8, and 24 hr after learning to escape to a novel location.

Acknowledgments

We would like to thank Dr. A. Kirkwood and Dr. D. Linden for kindly sharing equipment, C. Doherty for technical assistance, Dr. Y.-X. Wang for assistance on the immunogold labeling, and G. Sia for help with low-density hippocampal cultures. We thank A. Nagy for providing the R1 ES cells. We greatly appreciate D. Bury's help with the manuscript. This work was funded by the Howard Hughes Medical Institute, the Robert Packard Center for ALS Research (R.L.H.), and NIH grant R01 MH61108-02 (M.G.).

Received: July 29, 2002
Revised: January 15, 2003

References

Banke, T.G., Bowie, D., Lee, H., Huganir, R.L., Schousboe, A., and Traynelis, S.F. (2000). Control of GluR1 AMPA receptor function by cAMP-dependent protein kinase. J. Neurosci. *20*, 89–102.

Barria, A., Derkach, V., and Soderling, T. (1997a). Identification of the Ca^{2+}/calmodulin-dependent protein kinase II regulatory phosphorylation site in the α-amino-3-hydroxyl-5-methyl-4-isoxazolepropionate type gluatamate receptor. J. Biol. Chem. *272*, 32727–32730.

Barria, A., Muller, D., Derkach, V., Griffith, L.C., and Soderling, T.R. (1997b). Regulatory phosphorylation of AMPA-type glutamate receptors by CaM-KII during long-term potentiation. Science *276*, 2042–2045.

Beattie, E.C., Carroll, R.C., Yu, X., Morishita, W., Yasuda, H., von Zastrow, M., and Malenka, R.C. (2000). Regulation of AMPA receptor endocytosis by a signaling mechanism shared with LTD. Nat. Neurosci. *3*, 1291–1300.

Benke, T.A., Luthi, A., Isaac, J.T., and Collingridge, G.L. (1998). Modulation of AMPA receptor unitary conductance by synaptic activity. Nature *393*, 793–797.

Boulter, J., Hollmann, M., O'Shea-Greenfield, A., Hartley, M., Deneris, E., Maron, C., and Heinemann, S. (1990). Molecular cloning and functional expression of glutamate receptor subunit genes. Science *249*, 1033–1037.

Buonomano, D.V., and Merzenich, M.M. (1998). Cortical plasticity: from synapses to maps. Annu. Rev. Neurosci. *21*, 149–186.

Carroll, R.C., Lissing, D.V., von Zastrow, M., Nicoll, R.A., and Malenka, R.C. (1999). Rapid redistribution of glutamate receptors contributes to long-term depression in hippocampal cultures. Nat. Neurosci. *2*, 454–460.

Carroll, R.C., Beattie, E.C., von Zastrow, M., and Malenka, R.C. (2001). Role of AMPA receptor endocytosis in synaptic plasticity. Nat. Rev. Neurosci. *2*, 315–324.

Carvalho, A.L., Kameyama, K., and Huganir, R.L. (1999). Characterization of phosphorylation sites on the glutamate receptor 4 subunit of the AMPA receptors. J. Neurosci. *19*, 4748–4754.

Chung, H.J., Xia, J., Scannevin, R.H., Zhang, X., and Huganir, R.L. (2000). Phosphorylation of the AMPA receptor subunit GluR2 differentially regulates its interaction with PDZ domain-containing proteins. J. Neurosci. *20*, 7258–7267.

Daw, M.I., Chittajallu, R., Bortolotto, Z.A., Dev, K.K., Duprat, F., Henley, J.M., Collingridge, G.L., and Isaac, J.T. (2000). PDZ proteins interacting with C-terminal GluR2/3 are involved in a PKC-dependent regulation of AMPA receptors at hippocampal synapses. Neuron *28*, 873–886.

Derkach, V., Barria, A., and Soderling, T.R. (1999). Ca2+/calmodulin-kinase II enhances channel conductance of alpha-amino-3-hydroxy-5-methyl-4-isoxazolepropionate type glutamate receptors. Proc. Natl. Acad. Sci. USA *96*, 3269–3274.

Ehlers, M.D. (2000). Reinsertion or degradation of AMPA receptors determined by activity-dependent endocytic sorting. Neuron *28*, 511–525.

Esteban, J.A., Shi, S.H., Wilson, C., Nuriya, M., Huganir, R.L., and Malinow, R. (2003). PKA phosphorylation of AMPA receptor subunits controls synaptic trafficking underlying plasticity. Nat. Neurosci. *6*, 136–143.

Hayashi, Y., Shi, S.H., Esteban, J.A., Piccini, A., Poncer, J.C., and Malinow, R. (2000). Driving AMPA receptors into synapses by LTP and CaMKII: requirement for GluR1 and PDZ domain interaction. Science *287*, 2262–2267.

Hyman, S.E., and Malenka, R.C. (2001). Addiction and the brain: the neurobiology of compulsion and its persistence. Nat. Rev. Neurosci. *2*, 695–703.

Kameyama, K., Lee, H.-K., Bear, M.F., and Huganir, R.L. (1998). Involvement of a postsynaptic protein kinase A substrate in the expression of homosynaptic long-term depression. Neuron *21*, 1163–1175.

Keinanen, K., Wisden, W., Sommer, B., Werner, P., Herb, A., Verdoorn, T.A., Sakmann, B., and Seeburg, P.H. (1990). A family of AMPA-selective glutamate receptors. Science *249*, 556–560.

Kemp, N., McQueen, J., Faulkes, S., and Bashir, Z.I. (2000). Different forms of LTD in the CA1 region of the hippocampus: role of age and stimulus protocol. Eur. J. Neurosci. *12*, 360–366.

Kim, C.H., Chung, H.J., Lee, H.K., and Huganir, R.L. (2001). Interaction of the AMPA receptor subunit GluR2/3 with PDZ domains regulates hippocampal long-term depression. Proc. Natl. Acad. Sci. USA *98*, 11725–11730.

Lee, H.-K., Kameyama, K., Huganir, R.L., and Bear, M.F. (1998). NMDA induces long-term synaptic depression and dephosphorylation of the GluR1 subunit of AMPA receptors in hippocampus. Neuron *21*, 1151–1162.

Lee, H.-K., Barbarosie, M., Kameyama, K., Bear, M.F., and Huganir, R.L. (2000). Regulation of distinct AMPA receptor phosphorylation sites during bidirectional synaptic plasticity. Nature *405*, 955–959.

Lisberger, S.G. (1998). Cerebellar LTD: a molecular mechanism of behavioral learning? Cell *92*, 701–704.

Luscher, C., and Frerking, M. (2001). Restless AMPA receptors: implications for synaptic transmission and plasticity. Trends Neurosci. *24*, 665–670.

Mack, V., Burnashev, N., Kaiser, K.M.M., Rozov, A., Jensen, V., Hvalby, O., Seeburg, P.H., Sakmann, B., and Sprengel, R. (2001). Conditional restoration of hippocampal synaptic potentiation in GluR-A-deficient mice. Science *292*, 2501–2504.

Malenka, R.C., and Nicoll, R.A. (1999). Long-term potentiation–a decade of progress? Science *285*, 1870–1874.

Mammen, A.L., Kameyame, K., Roche, K.W., and Huganir, R.L. (1997). Phosphorylation of the α-amino-3-hydroxy-5-methylisoxazole-4-propionic acid receptor GluR1 subunit by calcium/calmodulin-dependent kinase II. J. Biol. Chem. *272*, 32528–32533.

Man, H.Y., Lin, J.W., Ju, W.H., Ahmadian, G., Liu, L., Becker, L.E., Sheng, M., and Wang, Y.T. (2000). Regulation of AMPA receptor-mediated synaptic transmission by clathrin-dependent receptor internalization. Neuron *25*, 649–662.

Martin, L.J., Blackstone, C.D., Levey, A.I., Huganir, R.L., and Price,

D.L. (1993). AMPA glutamate receptor subunits are differentially distributed in rat brain. Neuroscience *53*, 327–358.

Matsuda, S., Mikawa, S., and Hirai, H. (1999). Phosphorylation of serine-880 in GluR2 by protein kinase C prevents its C terminus from binding with glutamate receptor-interacting protein. J. Neurochem. *73*, 1765–1768.

McDonald, B.J., Chung, H.J., and Huganir, R.L. (2001). Identification of protein kinase C phosphorylation sites within the AMPA receptor GluR2 subunit. Neuropharmacology *41*, 672–679.

Morris, R.G.M., and Frey, U. (1997). Hippocampal synaptic plasiticity: role in spatial learning or the automatic recording of attended experience? Philos. Trans. R. Soc. Lond. B Biol. Sci. *352*, 1489–1503.

Nagy, A., Rossant, J., Nagy, R., Abramow-Newerly, W., and Roder, J. (1993). Derivation of completely cell culture-derived mice from early-passage embryonic stem cells. Proc. Natl. Acad. Sci. USA *90*, 8424–8428.

Nagy, A., Moens, C., Ivanyi, E., Pawling, J., Gertsenstein, M., Hadjantonakis, A.K., Pirity, M., and Rossant, J. (1998). Dissecting the role of N-myc in development using a single targeting vector to generate a series of alleles. Curr. Biol. *8*, 661–664.

Petralia, R.S., and Wenthold, R.J. (1992). Light and electron immunocytochemical localization of AMPA-selective glutamate receptors in the rat brain. J. Comp. Neurol. *318*, 329–354.

Petralia, R.S., and Wenthold, R.J. (1999). Immunocytochemistry of NMDA receptors. In Methods in Molecular Biology: NMDA Receptor Protocols, M. Li, ed. (Totowa, New Jersey: Humana Press), pp. 73–92.

Petralia, R.S., Esteban, J.A., Wang, Y.X., Partridge, J.G., Zhao, H.M., Wenthold, R.J., and Malinow, R. (1999). Selective acquisition of AMPA receptors over postnatal development suggests a molecular basis for silent synapses. Nat. Neurosci. *2*, 31–36.

Price, C.J., Kim, P., and Raymond, L.A. (1999). D1 dopamine receptor-induced cyclic AMP-dependent protein kinase phosphorylation and potentiation of striatal glutamate receptors. J. Neurochem. *73*, 2441–2446.

Reisel, D., Bannerman, D.M., Schmitt, W.B., Deacon, R.M.J., Flint, J., Borchardt, T., Seeburg, P.H., and Rawlins, J.N.P. (2002). Spatial memory dissociations in mice lacking GluR1. Nat. Neurosci. *5*, 868–873.

Roche, K.W., O'Brien, R.J., Mammen, A.L., Bernhardt, J., and Huganir, R.L. (1996). Characterization of multiple phosphorylation sites on the AMPA receptor GluR1 subunit. Neuron *16*, 1179–1188.

Sanes, J.N., and Donoghue, J.P. (2000). Plasticity and primary motor cortex. Annu. Rev. Neurosci. *23*, 393–415.

Shi, S.H., Hayashi, Y., Petralia, R.S., Zaman, S.H., Wenthold, R.J., Svoboda, K., and Malinow, R. (1999). Rapid spine delivery and redistribution of AMPA receptors after synaptic NMDA receptor activation. Science *284*, 1811–1816.

Shi, S., Hayashi, Y., Esteban, J.A., and Malinow, R. (2001). Subunit-specific rules governing AMPA receptor trafficking to synapses in hippocampal pyramidal neurons. Cell *105*, 331–343.

Snyder, G.L., Allen, P.B., Fienberg, A.A., Valle, C.G., Huganir, R.L., Nairn, A.C., and Greengard, P. (2000). Regulation of phosphorylation of the GluR1 AMPA receptor in the neostriatum by dopamine and psychostimulants in vivo. J. Neurosci. *20*, 4480–4488.

Song, I., and Huganir, R.L. (2002). Regulation of AMPA receptors during synaptic plasticity. Trends Neurosci. *25*, 578–588.

Squire, L.R. (1992). Memory and the hippocampus: a synthesis from findings with rats, monkeys, and humans. Psychol. Rev. *99*, 195–231.

Svenningsson, P., Tzavara, E.T., Witkin, J.M., Fienberg, A.A., Nomikos, G.G., and Greengard, P. (2002). Involvement of striatal and extrastriatal DARPP-32 in biochemical and behavioral effects of fluoxetine (Prozac). Proc. Natl. Acad. Sci. USA *99*, 182–187.

Zamanillo, D., Sprengel, R., Hvalby, O., Jensen, V., Brunashev, N., Rozov, A., Kaiser, K.M., Koster, H.J., Borchardt, T., Worley, P., et al. (1999). Importance of AMPA receptors for hippocampal synaptic plasticity but not for spatial learning. Science *284*, 1805–1811.

Zheng, H., Chattarji, S., Barbarosie, M., Rondi-Reig, L., Philpot, B.D., Miyakawa, T., Bear, M.F., and Tonegawa, S. (2001). Forebrain-specific calcineurin knockout selectively impairs bidirectional synaptic plasticity and working/episodic-like memory. Cell *107*, 617–629.